0026-895X/87/010091-09$02.00/0

MOLECULAR PHARMACOLOGY, 32:91–99

Muscarinic Receptor Heterogeneity in Rat Central Nervous System. I. Binding of Four Selective Antagonists to Three Muscarinic Receptor Subclasses: A Comparison with M2 Cardiac Muscarinic Receptors of the C Type

MAGALI WAELBROECK, MICHEL GILLARD, PATRICK ROBBERECHT, and JEAN CHRISTOPHE

Department of Biochemistry and Nutrition, Medical School, Université Libre de Bruxelles, B-1000 Brussels, Belgium (M.W., M.G., P.R., J.C.), and UCB Research Laboratories, Chemin Le Foriest, B-1420 Braine-l'Alleud, Belgium (M.G.)

Received December 4, 1986; Accepted April 14, 1987

SUMMARY

We previously observed that [^{3}H]NMS recognizes three types of muscarinic receptors in rat brain (one M1 subclass with high affinity for pirenzepine, and two M2 subclasses with low affinities for pirenzepine), based on distinct affinity and kinetic constants of [^{3}H]NMS for these three subclasses. In this work, we investigated the binding of four selective antagonists to these three (the M1 and two M2) subclasses. We were able to demonstrate that 1) cardiac-like M2 receptors with low affinity for pirenzepine and low affinity for *N*-methylscopolamine were present not only in cerebellum (as previously shown; see introduction) but also in cortex, striatum, and hippocampus, and 2) the two M2 receptor subclasses were discriminated by dicyclomine, 4-DAMP, and gallamine, as well as by AF-DX 116 and [^{3}H]NMS. Our findings also suggested that the biphasic association and dissociation kinetics of [^{3}H]NMS observed in various brain regions reflect sequential binding to the different receptors.

Increasing pharmacological and biochemical evidence suggests that there are at least three classes of muscarinic receptors.

In pharmacological studies, the antagonists 4-DAMP (1) and hexahydrosila-difenidol, and other derivatives (2) selectively block muscarinic responses in smooth muscle while having weaker action on cardiac muscarinic receptors. The allosteric antagonist gallamine (3, 4), like AF-DX 116 (5) and himbacine (6), present the reverse selectivity. Pirenzepine, by contrast, shows a similar low affinity for smooth muscle and cardiac receptors but detects high affinity receptors in the central and peripheral nervous system (7).

Pirenzepine selectivity is readily demonstrable in binding studies (8). Muscarinic receptors are, therefore, generally classified as M1 receptors with high affinity for pirenzepine and able to bind [^{3}H]pirenzepine, and M2 receptors are those with low affinity for unlabeled pirenzepine that do not recognize [^{3}H]pirenzepine. In addition, pirenzepine possesses an affinity slightly lower for cardiac M2 than for secretory gland M2 receptors (8), and in binding studies, competition curves using the pirenzepine analogue AF-DX 116 demonstrated the coexistence of two M2 receptors (9).

Our previous results (10) suggest that the so-called "nonselective" muscarinic antagonist [^{3}H]NMS detects three muscarinic receptor subclasses in rat brain, based on decreasing dissociation rates: 1) M2 C (or "cardiac-M2") receptors with a large [^{3}H]NMS dissociation rate (half-life: 1.5–2 min), 2) M1 A receptors with an intermediate [^{3}H]NMS dissociation rate (half-life of 7 min), and 3) M2 B (or "brain M2") receptors with a very low [^{3}H]NMS dissociation rate (half-life of 35 min) (10). Besides, [^{3}H]NMS possesses a higher affinity for brain M2 B receptors, followed by M1 A and cardiac M2 C receptors.

We hypothesized that brain M2 B receptors might be identical to the muscarinic receptors of smooth muscle and secretory glands, brain M2 C receptors being indentical to rat heart muscarinic receptors. Therefore, we tentatively adopted the nomenclature proposed by Birdsall *et al.* (11) on the basis of pirenzepine binding studies. If our hypothesis is correct, cardioselective rather than ileum-selective drugs would be necessary to demonstrate M2 receptor heterogeneity, due to the (small) selectivity of [^{3}H]NMS in binding studies. Indeed, high

This research was aided by Grant 3.4571.85 from the Fonds de la Recherche Scientifique Médicale (Belgium) and the Bekales Foundation (Liechtenstein).

ABBREVIATIONS: 4-DAMP, 4-diphenylacetoxy-*N*-methyl-piperidine methbromide; AF-DX 116, [11-{2-[(diethylamino)-methyl]-1-piperidinyl} acetyl)-5,11-dihydro-6H-pyrido(2,3-*b*) (1,4)benzodiazepin-6-on]; [^{3}H]NMS, [*N-methyl*-^{3}H]scopolamine methyl chloride; I_{50}, concentration of unlabeled drug necessary to inhibit 50% of tracer binding; K_i, unlabeled drug dissociation constant; K_D, tracer dissociation constant; k_{on}, association rate constant; k_{off}, dissociation rate constant.

[^{3}H]NMS concentrations are necessary to label correctly C receptors in systems containing B and C receptors, but, at these tracer concentrations, unlabeled drug binding to B receptors is more inhibited by competition with the tracer than unlabeled drug binding to C receptors. This effect of tracer might significantly decrease the apparent selectivity of B-preferring drugs (such as 4-DAMP, hexahydrosila-difenidol) while increasing the selectivity of C-preferring drugs (such as AF-DX 116).

To verify this hypothesis, we investigated the binding properties of four selective antagonists (pirenzepine, AF-DX 116, 4-DAMP, and dicyclomine) under various equilibrium and nonequilibrium conditions, to take advantage of the different kinetic and equilibrium binding properties of [^{3}H]NMS. The known binding and/or pharmacological characteristics of the four selective antagonists tested are as follows: a) pirenzepine is M1-selective in binding (8) and pharmacological (7) studies, it also presents a small preference for smooth muscle and secretory gland M2 receptors as compared to cardiac M2 receptors (8); b) AF-DX 116 is cardioselective in binding and pharmacological studies (5, 9, 12) with an intermediate affinity for M1 receptors and a lower affinity for parotid gland receptors (9, 12); c) 4-DAMP is an ileum-preferring antagonist in contraction studies (1); and d) dicyclomine is generally considered as M1-selective in binding studies (13), although it presents a greater affinity for parotid gland receptors as compared to heart receptors (two M2 receptor populations) in binding studies (13, 14).

Experimental Procedures

Materials. [^{3}H]NMS (specific radioactivity 74 Ci/mmol) was obtained from the Radiochemical Centre (Amersham, Bucks, England) and [^{3}H]pirenzepine (specific radioactivity 84 Ci/mmol) from New England Nuclear (Dreieich, FRG). The following drugs were gifts: pirenzepine (gastrozepin) from Dr. R. Hammer (Institute di Angeli, Milano, Italy), 4-DAMP from Dr. R. Barlow (University of Bristol Medical School, Bristol, England), and dicyclomine from Merrell-Dow (Brussels, Belgium). Dr. A. Giachetti (Institute di Angeli, Milano, Italy) helped us to obtain AF-DX 116 from Dr. K. Thomae GmbH (Biberach, FRG). Atropine and polyethyleneimine were from Sigma Chemical Co. (St. Louis, MO).

Methods. Male Wistar albino rats (200–250 g) fed rat chow *ad libitum* were killed by decapitation.

The cortex, hippocampus, striatum, and cerebellum were quickly dissected and homogenized in ice-cold homogenization buffer [20 mM Tris-HCl (pH 7.5) enriched with 0.25 M sucrose] using a glass-Teflon homogenizer. The homogenates [1% (w/v) for all [^{3}H]NMS binding studies; 5% (w/v) for [^{3}H]pirenzepine binding studies in cortex, hippocampus, and striatum; and 10% (w/v) for [^{3}H]NMS binding studies in cerebellum] were stored in liquid nitrogen until use.

The hearts were quickly removed, rinsed at room temperature in isotonic sodium chloride, and then homogenized in 3 ml of ice-cold homogenization buffer [20 mM Tris-HCl, (pH 7.5) enriched with 0.25 M sucrose] using an Ultraturrax homogenizer. The homogenate was diluted with the same buffer to 10% (w/v), filtered through two layers of medical gauze, and stored in liquid nitrogen until use.

All protein concentrations were determined using the method of Lowry *et al.* (15) with bovine serum albumin as standard.

Binding assays. Homogenates (400–500 μg of heart and cerebellum protein for [^{3}H]NMS binding; 30–40 μg of cortex, hippocampus, and striatum protein for [^{3}H]NMS binding; and 150–200 μg of cortex protein for [^{3}H]pirenzepine binding) were incubated for 2 hr at 25° in 1.2 ml of incubation buffer (50 mM sodium phosphate buffer, pH 7.4, enriched with 2 mM $MgCl_2$ and 1% bovine serum albumin) and the indicated concentrations of tracer and unlabeled drugs.

Specific binding was measured as follows. Each sample was filtered on GF/C glass-fiber filters (Whatman, Maidstone, England) presoaked in 0.05% polyethyleneimine, and then rinsed four times with 2 ml of ice-cold 50 mM sodium phosphate buffer (pH 7.4) (filters soaked in polyethyleneimine for at least 3 hr gave a lower nonspecific binding at large tracer concentration and a higher recovery of bound tracer at high protein concentration). The filters were dried and the radioactivity was counted by liquid scintillation. Nonspecific binding was defined as binding in the presence of 1 μM atropine. This radioactivity was subtracted from total binding, yielding specific binding.

[^{3}H]NMS-selective drug competition curves. Homogenates were incubated as explained above, in the presence of a constant [^{3}H]NMS or [^{3}H]pirenzepine concentration (see figure legends), and in the presence or absence of the indicated unlabeled drug concentrations or of 1 μM atropine. Specific binding was measured as mentioned above. The results were analyzed assuming that unlabeled drugs recognized one or two subclasses of muscarinic receptors with different I_{50} values, using a computer-assisted curve-fitting procedure [program developed by Richardson and Humrich (16)].

The fitted curves were within 2% of the experimental values, and are shown in Figs. 1–8 (see Results).

In equilibrium binding studies, the K_i values for unlabeled drugs were calculated according to the method of Cheng and Prusoff (17) for each receptor class:

$$I_i = K_i\left(1 + \frac{F}{K_D}\right)$$

with $i = 1$ to 3, where I_i is the I_{50} value of the unlabeled drugs for binding to class i receptors *at equilibrium*, F is the free tracer concentration, and K_i and K_D are the equilibrium dissociation constants of the unlabeled drugs and tracers for that receptor class.

The proportion of tracer bound in the absence of unlabeled drug was kept below 20% to prevent modification of F when the unlabeled drug concentration was increased.

Binding to the brain M1 A receptor subclass. The A receptor subclass has a high affinity for pirenzepine and is found in various brain regions. To study the unlabeled drugs' interaction with this receptor subclass only, we used [^{3}H]pirenzepine as tracer and cortex homogenates as receptor source. At the 5–7 nM tracer concentration used, [^{3}H]pirenzepine binding to B receptors was negligible in this brain area (see Ref. 10).

Binding to the brain M2 B receptor subclass. To investigate unlabeled drug interaction with the slowly dissociating M2 B receptors previously found in brain (10), we preincubated cortex homogenates with a low [^{3}H]NMS concentration and the unlabeled drugs for 2 hr, then added 1 μM atropine to induce tracer dissociation from A and C receptors. Tracer binding to B receptors was measured by filtration, after 35 min of isotopic dilution, as explained above.

Binding to the cardiac C receptor subclass. Muscarinic receptors in rat cardiac homogenates behave as a homogeneous receptor subclass in kinetic studies (10). We therefore used this tissue as a model to study the unlabeled drugs' interaction with C receptors. [^{3}H]NMS was used as tracer since pirenzepine has a very low affinity for these receptors.

Pulse experiments. In some experiments the homogenates were preincubated for 2 hr with the unlabeled drugs, to allow full equilibration. Tracer ([^{3}H]NMS) addition was delayed until 1 min before either immediate filtration ("pulse" experiments) or 1 μM atropine addition. For "pulse-chase" experiments, atropine addition was followed by another 12-min incubation before filtration, to allow full dissociation of the tracer bound to C receptors.

Results

Binding of five muscarinic antagonists to A, B, and C receptors. We have previously demonstrated that secoverine is a truly nonselective antagonist (18), i.e., a drug unable to

differentiate (under our incubation conditions) the A, B, and C receptor subclasses and the cardiac receptor states with high, low, and very low affinity for agonists (similar to brain SH, H, and L receptors, respectively). The K_i value of secoverine is 4–5 nM in all of these systems (18), and this is why we included this molecule as a reference.

As shown in Fig. 1 and Table 1, none of the antagonists studied could be used to identify simultaneously the three receptor subtypes in our incubation conditions: each of them recognized two out of three receptor subclasses with very similar affinities.

Pirenzepine was clearly A-preferring, and had a slightly (about 4-fold) greater affinity for B rather than C receptors. 4-DAMP and dicyclomine did not differentiate A and B receptors, but had a significantly lower affinity for C receptors. AF-DX 116 presented the reverse selectivity: C > A = B.

Gallamine (gallamine triethiodide) inhibits the association of [^{3}H]oxotremorine-M and [^{3}H]NMS (19) and that of [^{3}H]

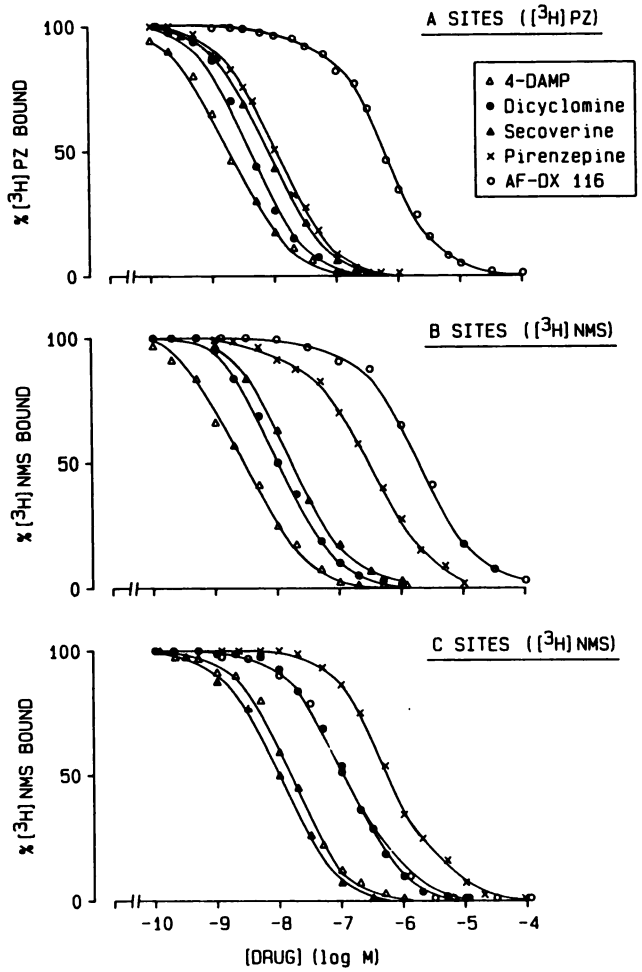

Fig. 1. Competition curves of 4-DAMP (△), dicyclomine (●), secoverine (▲), pirenzepine (×), and AF-DX 116 (○) for A receptors (*top*), B receptors (*middle*), and C receptors (*bottom*). The three muscarinic antagonist receptor subclasses were labeled separately as explained under Experimental Procedures: binding to the brain M1 A, brain M2 B, and cardiac C receptor subclasses. The tracer concentrations used corresponded to 1 K_D value for A receptors (6 nM [^{3}H]pirenzepine), 2.5 K_D value for B receptors (240 pM [^{3}H]NMS), and 1 K_D value for C receptors (500 pM [^{3}H]NMS). Average of three to seven experiments.

TABLE 1

pA_2 (−log K_i) and K_i values (in parentheses) of muscarinic antagonists for A, B, and C receptors (from Fig. 1)[a]

Antagonist	A receptors	B receptors	C receptors
Secoverine	8.3 (5 nM)	8.2 (6 nM)	8.3 (5 nM)
4-DAMP	9.0 (1 nM)	9.1 (0.9 nM)	8.1 (8 nM)
Dicyclomine	8.6 (2.5 nM)	8.5 (3 nM)	7.2 (60 nM)
Pirenzepine	8.3 (5 nM)	7.1 (80 nM)	6.5 (350 nM)
AF-DX 116	6.2 (600 nM)	6.3 (500 nM)	7.3 (50 nM)
Gallamine[b]	6.2 (0.6 μM)	5.5 (3 μM)	7.0 (0.1 μM)

[a] The standard deviations of pA_2 values were below 0.2 for binding to A and C receptors, and below 0.3 for binding to B receptors.

[b] K_i values given for gallamine refer to inhibition of muscarinic drugs' *association* to muscarinic receptors. The K_i for A receptors was measured with [^{3}H]pirenzepine in various brain regions (20, 21); K_i values for B receptors were measured with [^{3}H] oxotremorine-M in cortex and heart homogenates [see the accompanying paper (20)]; K_i values for C receptors were measured with [^{3}H]NMS and [^{3}H]oxotremorine-M in heart and cortex homogenates (19, 20).

quinuclidinyl benzilate[1] with the same potency when cardiac C receptors are considered. This suggests that the effect of gallamine on the association (but not dissociation) of muscarinic drug is independent of the tracer used. In the present study, we were unable to study the interaction of gallamine with B receptors in cortex using [^{3}H]NMS binding, due to its effect on the dissociation rate of the tracer from the three receptor types. We will demonstrate in the accompanying paper (20) that gallamine has a lower affinity for B receptors labeled by [^{3}H] oxotremorine-M than for A (20, 21) and C receptors (4, 19–21) (Table 1).

In summary, three selectivity patterns were observed in our experiments: A > B > C (for pirenzepine), B, A > C (for 4-DAMP and dicyclomine), and C > A, B (for AF-DX 116). Gallamine (Table 1 and Ref. 20) showed a fourth selectivity pattern: C > A > B.

Equilibrium [^{3}H]NMS competition curves. We compared selective drug-[^{3}H]NMS competition curves obtained at equilibrium and at two tracer concentrations (0.25 and 2.5 nM [^{3}H]NMS) with cortex, cerebellum, and heart homogenates (Figs. 2–5).

As shown in Fig. 2, pirenzepine competition curves obtained at two tracer concentrations were parallel, a result compatible with nonselective tracer binding in the three homogenates. Pirenzepine and [^{3}H]NMS had a low affinity for cardiac and cerebellum receptors, as indicated by a high I_{50} value for pirenzepine and by the small rightward shift of competition curves at high tracer concentration. Pirenzepine recognized two types of receptors in cortex: M1 receptors with an apparent K_i value of 6 nM and M2 receptors with an apparent K_i value (120 nM) smaller than that for heart and cerebellum M2 receptors (350 and 250 nM, respectively). [^{3}H]NMS had a greater affinity for both M1 and M2 cortex receptors, as indicated by a greater rightward shift of pirenzepine competition curves at high tracer concentration. The effective pirenzepine selectivity (ratio of "M2" I_{50} values, see legend of Fig. 2) was not sufficient, in the presence of [^{3}H]NMS, to detect M2 receptor heterogeneity by this method.

4-DAMP and dicyclomine had a greater affinity for cortex than for heart and cerebellum receptors, as indicated by a smaller I_{50} value in cortex at low tracer concentration (Fig. 3). The effective selectivity (ratio of I_{50} values in heart and cortex)

[1] M. Waelbroeck, M. Gillard, P. Robberecht, and J. Christophe, unpublished data.

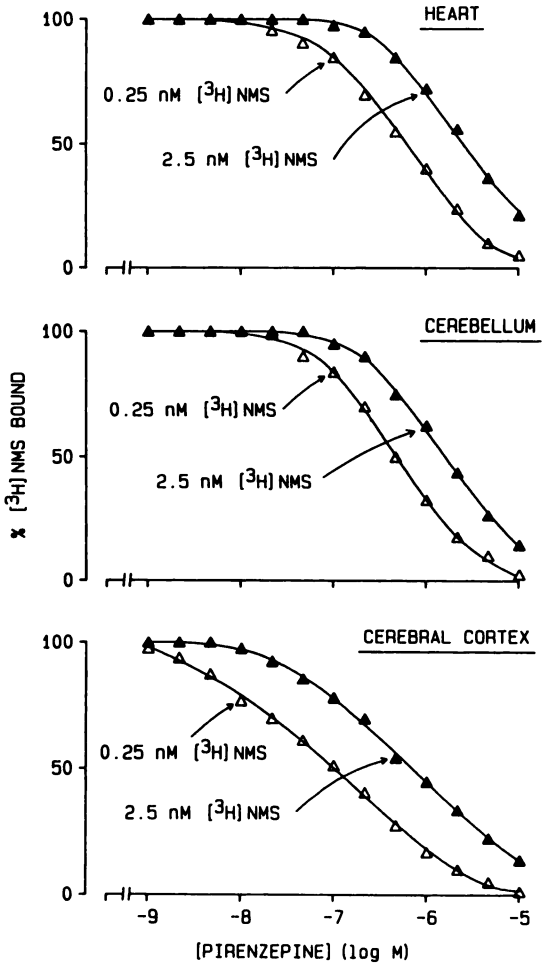

Fig. 2. Pirenzepine/[^{3}H]NMS competition curves were obtained in cardiac (*top*), cerebellar (*middle*), and cortical (*bottom*) homogenates, using 0.25 nM (△) and 2.5 nM (▲) [^{3}H]NMS. Hill coefficients of competition curves were 1.0 ± 0.1 in heart and cerebellum, 0.7 ± 0.1 in cortex. In this experiment, pirenzepine I_{50} values increased with the [^{3}H]NMS concentration from 0.6 to 2.5 μM in heart, 0.5 to 2.0 μM in cerebellum, and from 12 nM (M1)/0.4 μM (M2) to 100 nM (M1)/2.2 μM (M2) in cortex [assuming that 42% of receptors labeled at both tracer concentrations (the M1 receptors) had a high pirenzepine affinity]. The effective pirenzepine selectivity (heart M2/cortex M2 I_{50} ratio) decreased from 1.5 to 1.1 with increasing [^{3}H]NMS. Representative of three experiments.

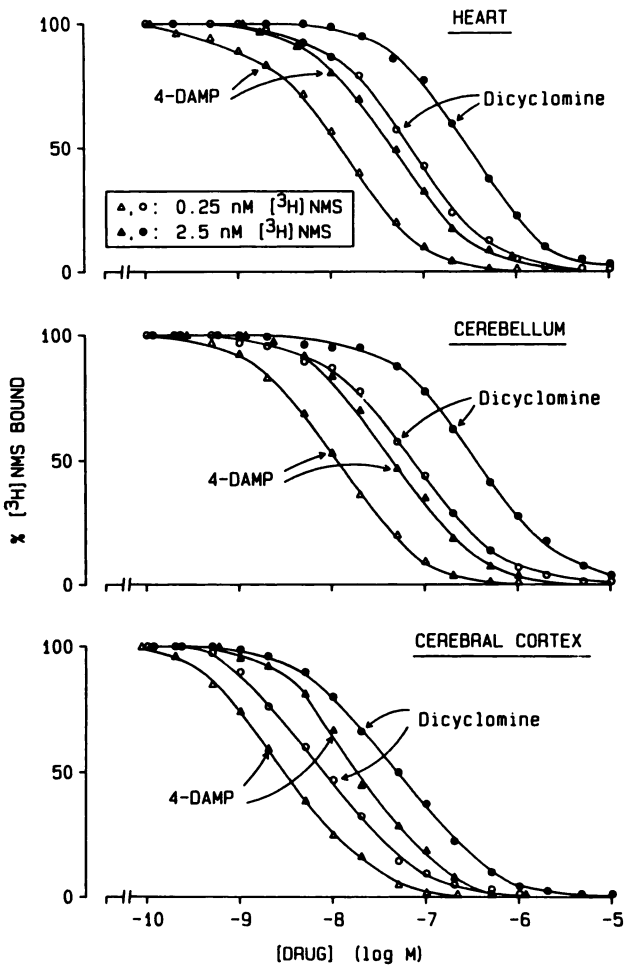

Fig. 3. As in Fig. 2, using 4-DAMP (▲, △) or dicyclomine (●, ○) instead of pirenzepine as unlabeled ligand, and using 0.25 nM (○, △) or 2.5 nM (●, ▲) [^{3}H]NMS. In cerebellum and heart, Hill coefficients of 4-DAMP competition curves were equal to 1.0 ± 0.1. In cortex, Hill coefficients were 1.0 ± 0.1 for 4-DAMP, and 0.9 ± 0.1 for dicyclomine. All competition curves were therefore analyzed assuming one receptor class only. In this experiment, the 4-DAMP I_{50} increased from 13 to 50 nM (heart), 11 to 40 nM (cerebellum), and 3 to 16 nM (cortex) with increasing tracer concentration. The dicyclomine I_{50} increased from, respectively, 75 to 300 nM (heart), 65 to 300 nM (cerebellum), and 8 to 50 nM (cortex). Effective selectivities of 4-DAMP and dicyclomine decreased with increasing [^{3}H]NMS concentration from, respectively, 4.3 to 3.1 and 9 to 6. Representative of three experiments.

decreased with increasing tracer concentration so that these molecules could not be used to detect M2 receptor heterogeneity at the high tracer concentration necessary to label a significant proportion of C receptors in cortex (10) (see legend of Fig. 3). Since 4-DAMP and dicyclomine had the same K_i value for A and B receptors (Table 1), these antagonists could not be used to detect receptor heterogeneity in [^{3}H]NMS equilibrium binding studies, at least under our incubation conditions.

As indicated above (see Fig. 1), AF-DX 116 had a homogeneous high affinity for heart receptors. By contrast, AF-DX 116 competition curves obtained in cerebellum and cortex were biphasic and shifted in a nonparallel fashion by increasing [^{3}H] NMS concentration (Hill coefficients varied by about 0.2 unit; legend of Fig. 4): AF-DX 116 selectivity and the proportion of high AF-DX 116 affinity sites labeled by [^{3}H]NMS increased with increasing tracer concentration (see legend of Fig. 4). These results indicated that [^{3}H]NMS recognized with a lower affinity a receptor subclass having a high affinity for AF-DX 116, both in cerebellum and cortex.

We analyzed AF-DX 116 and pirenzepine competition curves obtained at low and high tracer concentrations (Figs 2, 4, and 5, and data not shown). The results indicated that [^{3}H]NMS used in saturating concentrations could label, respectively, 25 ± 5, 20 ± 5, 15 ± 4, and 90 ± 5% of C receptors in cortex, hippocampus, striatum, and cerebellum. In the same brain areas, [^{3}H]NMS labeled, respectively, 40 ± 5, 55 ± 10, 25 ± 5%, and undetectable levels of A receptors (not shown).

The proportions of C receptors obtained in this work were in good agreement with those expected from dissociation kinetics (10), except in striatum. The discrepancy in the latter case presumably reflected our previous difficulty in fitting simultaneously pirenzepine equilibrium competition curves and [^{3}H] NMS dissociation kinetics, at low and high tracer concentrations: we had probably underestimated the proportion of A receptors labeled at high [^{3}H]NMS concentration in striatum

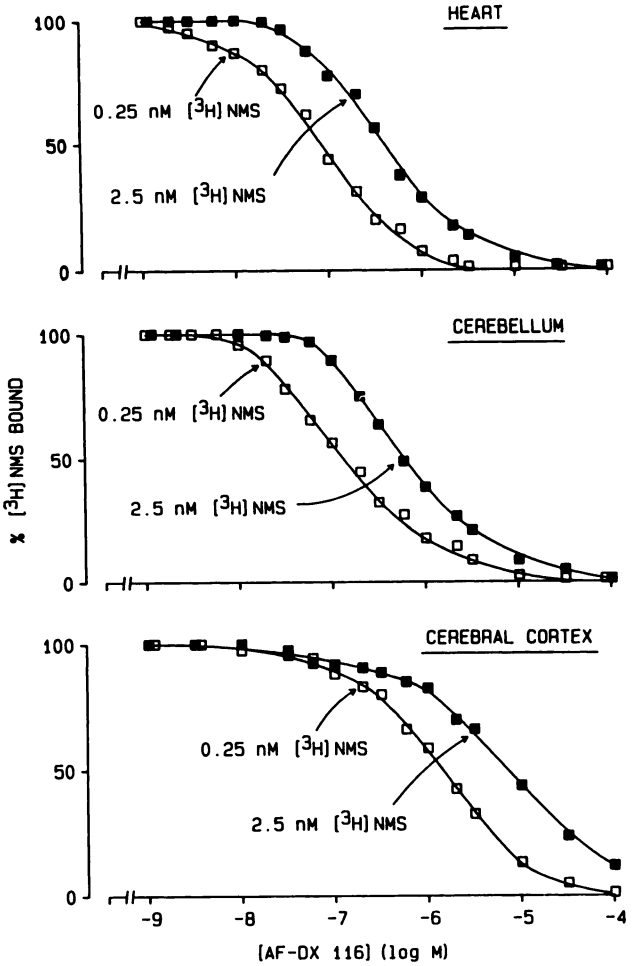

Fig. 4. As in Fig. 2, using AF-DX 116 instead of pirenzepine as unlabeled ligand. Hill coefficients of AF-DX 116 competition curves were 1.0 ± 0.1 at both tracer concentrations in heart homogenates. In cerebellum and cortex homogenates, Hill coefficients varied from, respectively, 0.73 to 0.91 (±0.1) and from 0.85 to 0.66 (±0.1) with increasing tracer concentration. All competition curves were compatible with the existence of two receptor subclasses, with [^{3}H]NMS K_D and AF-DX 116 K_i values of, respectively, 500 pM/50 nM and 100 pM/0.6 μM. Indeed, the [^{3}H]NMS labeling of sites with high affinity for AF-DX 116 increased from 75 to 85% in cerebellum and from 11 to 23% in cortex with increasing [^{3}H] NMS concentration. AF-DX 116 I_{50} increased from 80 nM to 410 nM (cardiac and high affinity receptors in cortex and cerebellum) and 1.6 μM to 13.0 μM (low affinity receptors in cerebellum and cortex) when tracer concentration increased from 0.25 to 2.5 nM. Effective AX-DX 116 selectivity (cortex low affinity/heart I_{50} ratio) increased from 20 to 32 with increasing [^{3}H]NMS concentration. Representative of three to five experiments.

homogenates, therefore attributing all tracer dependence of dissociation kinetics to the labeling of C receptors.

Pulse experiments. [^{3}H]NMS binding to C sites was very low, at equilibrium. The above results were fully compatible with the hypothesis that cardiac and brain C receptors had identical binding properties. However, we were worried, since AF-DX 116 was the only antagonist detecting C sites unambiguously in brain, and determining its I_{50} value at low tracer concentration was not precise due to low tracer binding to this subsite. At higher tracer concentrations, the I_{50} value estimate was more reliable, but estimates of the unlabeled drug K_i value depend heavily on the tracers' K_D value (17)—another difficulty in this system. We therefore sought a method that would make the Cheng and Prusoff equation (17) unnecessary and increase [^{3}H]NMS binding to C sites.

We previously observed that [^{3}H]NMS has a lower affinity, and greater association and dissociation rates for C than for A and B receptors. It was theoretically possible, therefore, to favor [^{3}H]NMS binding to C receptors in rat brain by using short incubation periods with high tracer concentration.

To avoid unlabeled drug equilibration problems, we decided to preincubate cortex and heart homogenates for 2 hr with the drugs and without tracer. Under these conditions, the drugs occupied muscarinic receptors according to their K_i values (see below). By choosing thereafter a very short tracer incubation period, we ensured that: 1) unlabeled drugs would have little time to dissociate from receptors, and 2) receptor occupancy by [^{3}H]NMS would be low, mimicking a very low tracer concentration. Binding inhibition would then reflect unlabeled drug K_i values, rather than an I_{50} value affected by [^{3}H]NMS affinity (17). We therefore expected to be able to demonstrate the selectivity of not only C-preferring but also B-preferring drugs, and to avoid the errors inherent to large "Cheng-Prusoff" corrections when estimating the AF-DX 116, dicyclomine, and 4-DAMP K_i values. By contrast, the estimated proportions of A, B, and C receptors labeled by [^{3}H]NMS were likely to reflect not only the receptor proportions but *also* association and dissociation rates, as discussed below.

We had previously found [^{3}H]NMS K_D and k_{off} values of, respectively, 150–200 pM and 0.1 min^{-1} for A receptors, 50–100 pM and 0.02 min^{-1} for B receptors, and 500 pM and 0.35 min^{-1} for C receptors.

We assumed that, as in cardiac membranes (19), [^{3}H]NMS binding to each receptor subclass was adequately described by a one-step reaction. Using the equation $K_D = k_{off}/k_{on}$, we expected k_{on} values equal to 0.7–0.5 $nM^{-1}\cdot min^{-1}$ for A receptors, 0.4–0.2 $nM^{-1}\cdot min^{-1}$ for B receptors, and 0.7 $nM^{-1}\cdot min^{-1}$ for C receptors. We utilized these K_D, k_{on}, and k_{off} values to calculate the expected proportions of A, B, and C receptors labeled by [^{3}H]NMS after pulse, pulse-chase, and equilibrium incubations, using the following equations for each receptor type:

at equilibrium

$$B = RF/(K_D + F) \quad (1)$$

where B represents tracer binding to the receptor at equilibrium, K_D and F represent the [^{3}H]NMS equilibrium dissociation constant and free tracer concentration, and R is the receptor concentration.

after 1-min incubations (pulse experiments)

$$B_{1\ min} = B\, e^{(k_{on} F + k_{off})\ 1\ min} \quad (2)$$

where $B_{1\ min}$ represents tracer binding after 1 min of incubation.

in pulse chase experiments

$$B_{1/12\ min} = B_{1\ min}\, e^{-12\ min\ k_{off}} \quad (3)$$

where $B_{1/12\ min}$ represents tracer binding after 1 min association followed by 12 min of dissociation (pulse-chase).

On this theoretical ground, the proportions of [^{3}H]NMS binding expected for each receptor subclass varied markedly after 1 min incubation (but not at equilibrium) with the combination of K_D values chosen (not shown). Labeling of A and C receptors was systematically favored by short incubations.

The results of pulse experiments (Figs. 6–8) were in very

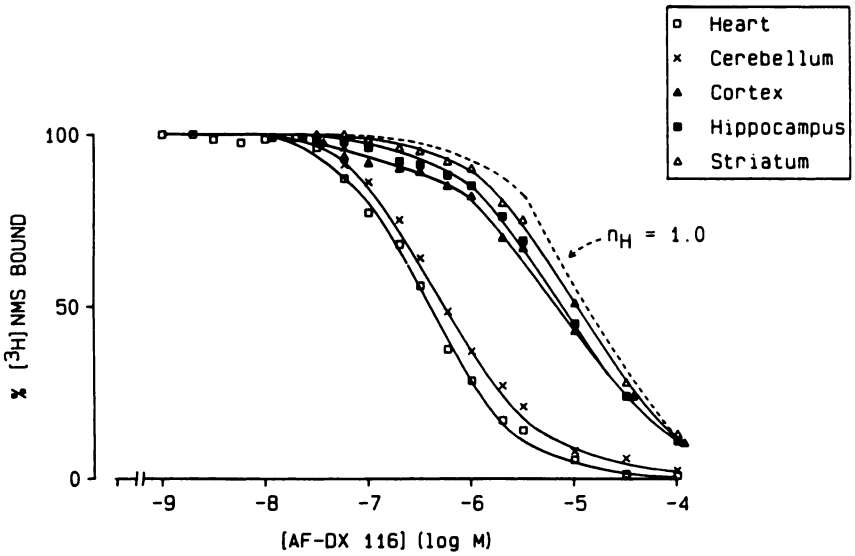

Fig. 5. AF-DX 116/[^{3}H]NMS competition curves in heart (□), cerebellum (×), cortex (▲), hippocampus (■), and striatum (△) homogenates obtained at 2.5 nM [^{3}H]NMS. High AF-DX 116 affinity receptors (I_{50} value: 0.3 ± 0.05 μM) represented, respectively, 100, 89 ± 4, 23 ± 5, 18 ± 4, and 13 ± 4% of [^{3}H]NMS binding, the remaining receptors having an I_{50} of 14 ± 4 μM. ---, a competition curve with a Hill coefficient (n_H) = 1.0 and I_{50} of 14.0 μM. Average of 5–10 experiments.

good agreement with those expected, admitting as [^{3}H]NMS K_D values of 150, 80, and 500 pM for, respectively, A, B, and C receptors. Indeed, 1) in pulse experiments competition curves by all selective antagonists were biphasic in brain (Figs. 6–8); 2) I_{50} values of 4-DAMP (not shown), dicyclomine (Fig. 7), and AF-DX 116 (Fig. 8) corresponded to their K_i values for A = B, and C receptors, respectively, in brain and to their K_i values in heart. Pirenzepine I_{50} values in brain corresponded to its K_i value for A receptors (Fig. 6), and to an average B-C K_i value (Fig. 6). It was equal to its "C" K_i value in heart (Fig. 6). 3) The proportion of [^{3}H]NMS-labeled C receptors (with a low I_{50} value for AF-DX 116 and a high I_{50} value for dicyclomine and 4-DAMP) was in conformity with the expected values (Figs. 6–8, Table 2). 4) We performed "pulse-chase" incubations, in order to eliminate the [^{3}H]NMS labeling of C receptors [labeling of A, B, and C receptors decreased by 70, 21, and 98%, respectively, after 12 min isotopic dilution (12)]. The expected and experimental results were again quantitatively in line: [^{3}H]NMS labeling of A and B receptors was close to the expected value, and selective drug I_{50} values corresponded to their K_i values for A and B receptors (Figs. 6–8, Table 2). Thus, cardiac and brain C receptors had the same kinetic and equilibrium binding properties.

Discussion

The existence of three muscarinic receptor subclasses is supported by an increasing number of pharmacological studies, as discussed in the introduction (1, 2, 4–7). Pirenzepine and AF-DX 116 are, however, the only molecules known to allow the detection of receptor heterogeneity in equilibrium binding studies, using [^{3}H]NMS (8, 9): pirenzepine distinguishes clearly A from B-C receptors; AF-DX 116 recognizes preferentially C as compared to A-B receptors (8, 9, 11, 12).

We previously suggested that [^{3}H]NMS recognizes three muscarinic receptor subclasses with different affinities, and association and dissociation rate constants in various rat brain regions (10). The M1 or A receptors have an intermediate affinity for [^{3}H]NMS (K_D 150 pM), an intermediate dissociation rate constant (0.1 min^{-1}), and a large affinity for pirenzepine (K_D 6 nM). An M2 receptor subclass found predominantly in forebrain has a high affinity for [^{3}H]NMS (K_D 80 pM), a very low [^{3}H]NMS dissociation rate constant (0.02 min^{-1}), and a low affinity for pirenzepine (K_D 80 nM). These brain M2 B receptors differ markedly from cardiac M2 C receptors, which have a lower affinity for [^{3}H]NMS (K_D 500 pM), a large [^{3}H]NMS dissociation rate constant (0.35 min^{-1}), and a lower affinity for pirenzepine (K_D 350 nM) (Ref. 10 and this work).

Here, using AF-DX 116, we confirmed that three receptor subtypes coexist in rat brain. The proportions of C receptors found in this work were in reasonable agreement with our previous estimate from kinetic studies in cortex, hippocampus, and cerebellum.

When studying separately the A, B, and C receptors (see Fig. 1 and Table 1), we observed that dicyclomine and 4-DAMP, like AF-DX 116, distinguished C receptors from A and B receptors. Four patterns of selectivity were characterized (Table 1): a) pirenzepine was A-preferring, b) dicyclomine and 4-DAMP were A-B preferring, c) AF-DX 116 was C-preferring, and d) gallamine presented a small C > A > B selectivity (20).

[^{3}H]NMS also showed a low selectivity, comparable to the dicyclomine and 4-DAMP pattern, with B > A > C. At equilibrium, we could not use dicyclomine and 4-DAMP to demonstrate receptor heterogeneity, due to this [^{3}H]NMS selectivity. Indeed, a large tracer concentration was needed to avoid underestimating C receptors (see Fig. 4), but this maneuver decreased the effective selectivity of B-preferring antagonists (see Fig. 3).

Pirenzepine detected readily the M1/M2 receptor heterogeneity under equilibrium conditions. The results obtained at different tracer concentrations indicated that [^{3}H]NMS had the same average affinity for M1 and M2 receptors. Indeed, the proportion of [^{3}H]NMS bound to M1 receptors did not change with tracer concentration (Fig. 2).

AF-DX 116 also readily detected receptor heterogeneity in cerebellum, cortex, hippocampus, and striatum (Fig. 5). In these four regions the proportion of labeled high AF-DX 116 affinity receptors: 1) increased with increasing [^{3}H]NMS concentration (Fig. 4 and results not shown), and 2) did not correlate with the proportion of either M1 or M2 receptors found with pirenzepine (Figs. 2 and 4).

These results, together with those in Fig. 1, confirmed that [^{3}H]NMS labeled all three muscarinic receptor subclasses in

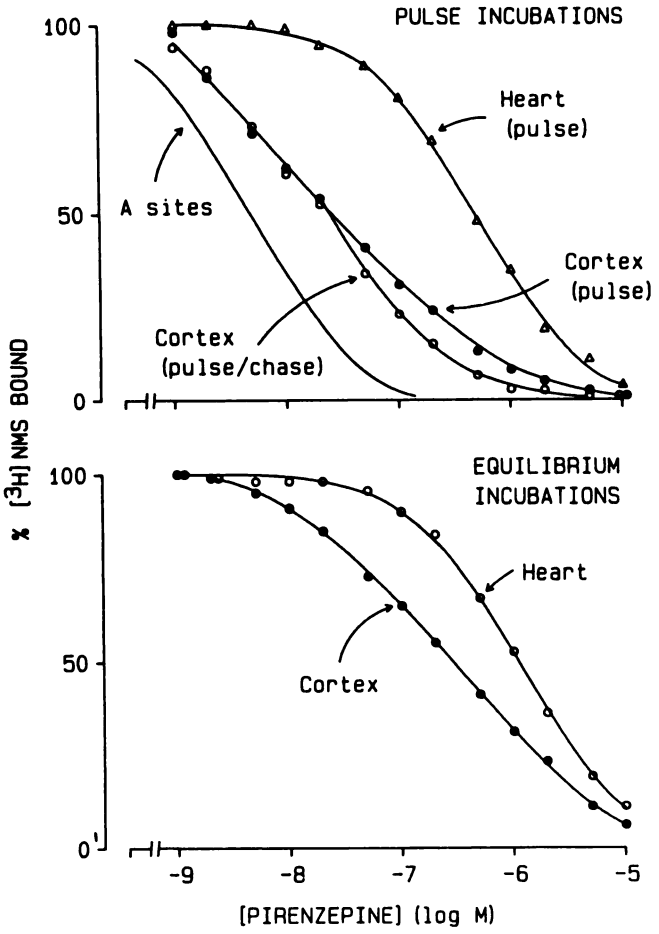

Fig. 6. Pirenzepine/[^{3}H]NMS competition curves in cerebral cortex (○, ●) and heart (△) obtained at 1.0 nM [^{3}H]NMS. Three incubation protocols were followed. *Top*. "Pulse" incubations: [^{3}H]NMS was allowed to interact for only 1 min (●, △) with brain or heart homogenates (preequilibrated with the indicated pirenzepine concentrations. "Pulse-chase" incubations: [^{3}H]NMS was allowed to bind to cortex homogenates for only 1 min (as for pulse incubations), followed by a 12-min isotopic dilution to eliminate tracer binding to C receptors (○). *N.B. A sites* (—): pulse [^{3}H]NMS binding to high affinity pirenzepine receptors (site with I_{50} of 6 nM) is shown for comparison with total binding. *Bottom*. "Equilibrium" incubations: [^{3}H]NMS was added simultaneously with the unlabeled drug at the beginning of the 2-hr incubation. All pirenzepine competition curves in cortex were significantly better fitted by a two-receptor subclass model. Pirenzepine I_{50} values were, respectively: in "pulse" experiments, 6 nM (57% of cortex labeling), 170 nM (43% of cortex labeling), and 400 nM (100% of heart labeling); in "pulse-chase" experiments (in cortex only), 6 nM (52% of residual labeling) and 80 nM (48% of residual labeling); and in "equilibrium" experiments, 35 nM (43% of cortex labeling), 900 nM (57% of cortex labeling), and 1100 nM (100% of cardiac labeling). Averages of four to eight experiments.

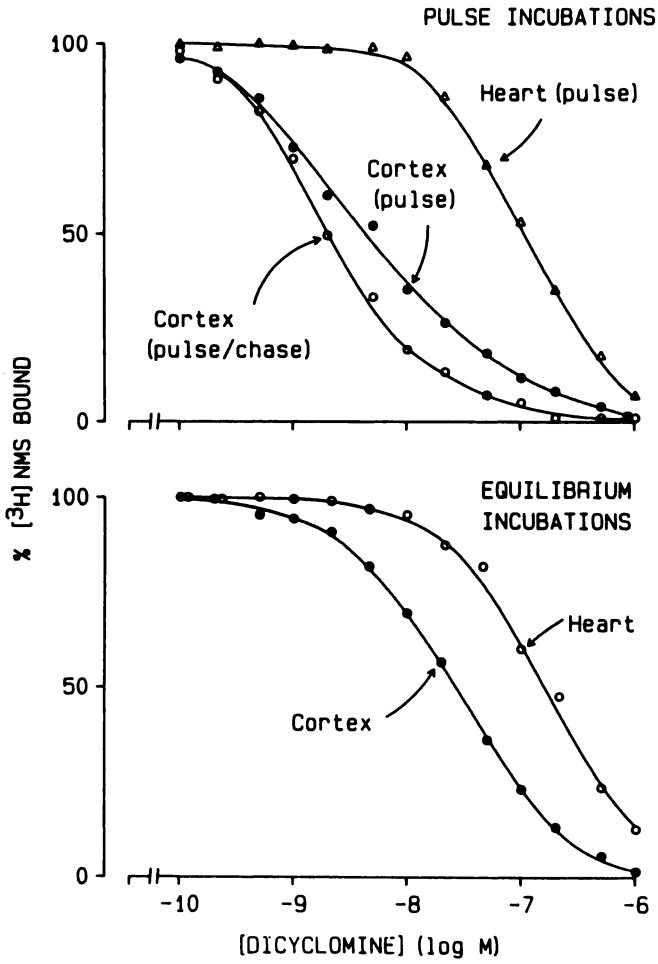

Fig. 7. Dicyclomine/[^{3}H]NMS competition curves in cortex (○, ●) and heart (△) homogenates. "Pulse" (*top*), "pulse-chase" (*top*), and equilibrium (*bottom*) experiments were performed as for Fig. 5. Competition curves obtained in "pulse" experiments only were significantly better fitted when assuming two receptors. Dicyclomine I_{50} values were, respectively: in "pulse" experiments, 2 nM (75% of cortex labeling), 70 nM (25% of cortex labeling), and 100 nM (100% of heart labeling); in "pulse-chase" experiments, 2.6 nM (100% of residual cortex labeling); and in equilibrium experiments, 26 nM (100% of cortex labeling) and 170 nM (100% of heart labeling). Average of three to eight experiments. Similar results were obtained in parallel experiments (not shown for clarity) using 4-DAMP. 4-DAMP I_{50} values were, respectively: in "pulse" experiments, 0.8 nM (70%) of cortex labeling, 8 nM (30% of cortex labeling), and 8 nM (100% of heart labeling); in "pulse-chase" experiments, 0.7 nM (100% of residual cortex labeling); and in equilibrium experiments, 9 nM (100% of cortex labeling) and 23 nM (100% of heart receptors). Average of three to eight experiments.

cortex. [^{3}H]NMS had a greater affinity for one of the two M2 receptors (80 pM) and a lower affinity for the second type of M2 receptors (500 pM). Therefore, its measured "average M2 affinity" on a log scale (150 pM) was similar to its affinity for M1 receptors (120 pM).

After prolonged incubation (i.e., under equilibrium conditions), [^{3}H]NMS binding to B receptors was favored. This made the observation of C receptors difficult. Since we expected that C receptors would be overlabeled if large [^{3}H]NMS concentrations were allowed to bind to cortex muscarinic receptors for only very short periods of time (see Table 2), we decided to investigate the binding of unlabeled drugs to cortex receptors under nonequilibrium conditions. This allowed us to demonstrate clearly the coexistence of: 1) a rapidly labeled receptor subclass with low affinity for pirenzepine, dicyclomine, and 4-DAMP, and high affinity for AF-DX 116; 2) a second receptor subclass with low affinity for pirenzepine and AF-DX 116, and high affinity for 4-DAMP and dicyclomine; and 3) a third receptor subclass with high affinity for pirenzepine, 4-DAMP, and dicyclomine, and low affinity for AF-DX 116. [^{3}H]NMS bound to these three receptors with different association rates.

Similarity of three muscarinic receptor subclasses with pharmacologically defined receptors. Muscarinic receptors with selectivities somewhat similar to those of the A, B, and C sites described here have been detected in pharmacological studies. Receptors with high affinity for pirenzepine

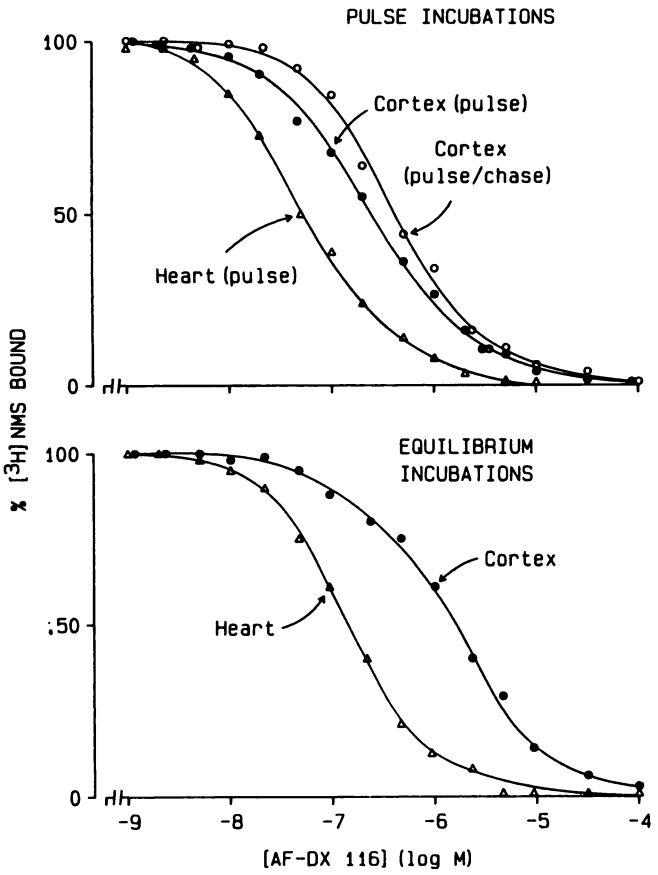

Fig. 8. AF-DX 116/[^{3}H]NMS competition curves were obtained in cortex (○, ●) and heart (△) as in Fig. 6. Competition curves obtained in cortex, pulse, and equilibrium incubations, only, were significantly better fitted by a two-receptor model. AF-DX 116 I_{50} values were, respectively: in "pulse" experiments, 40 nM (27% of cortex labeling), 550 nM (73% of cortex labeling), and 60 nM (100% of heart labeling); in "pulse-chase" experiments, 510 nM (100% of residual cortex labeling); and in equilibrium experiments, 160 nM (15% of cortex labeling), 5.0 μM (85% of cortex labeling), and 160 nM (100% of cardiac labeling). Average of four to nine experiments.

(similar to A receptors?) With pA_2 above 8.0) are responsible for depolarization or increased K^+ conductance in the central nervous system as well as in some peripheral nerves (22, 23). These receptors also have a high affinity for 4-DAMP (pA_2 8.7). Receptors responsible for smooth muscle contraction (B receptors?) and for cardiac contractility (C receptors?) both have a low affinity for pirenzepine (pA_2 6.2–7.0) (4). They can be differentiated *inter alia*, by their affinities for 4-DAMP (a B-preferring competitive antagonist) and for gallamine (a C-preferring allosteric antagonist). pK_a values of 4-DAMP (ileum, 8.4; atria, 7.6) (1), AF-DX 116 (ileum, 6.4; atria, 7.3) (5), and gallamine (ileum, <3–4.7; atria, 5.7–5.9) (reviewed in Ref. 5) in pharmacological studies compare favorably with their relative log K_i values for B and C receptors, respectively (see Table 1). Our K_i values were obtained in a nonphysiological buffer at a low (25°) temperature to allow comparison with our previous results, and this might explain the moderate differences between the above pA_2 values and our K_i values. If this is true, the three muscarinic binding sites described in this work correspond to three functionally distinct muscarinic receptors, as opposed to receptor "states" or non-receptor-binding sites. Measurements of the K_i values of selective drugs under more

TABLE 2

Comparison of expected and measured [^{3}H]NMS binding to A, B, and C receptors under various incubation conditions

[^{3}H]NMS (1 nM) binding to each site was calculated at equilibrium, after 1 min association (pulse), and after 1 min binding followed by 12 min dissociation (pulse-chase), using the following parameters: [^{3}H]NMS, 1 nM; A sites, 45%, k_{on} = 0.67 $nM^{-1}\cdot min^{-1}$; k_{off} = 0.1 min^{-1}; B sites, 35%, k_{on} = 0.25 $nM^{-1}\cdot min^{-1}$, k_{off} = 0.02 min^{-1}; C sites, 20%, k_{on} = 0.70 $nM^{-1}\cdot min^{-1}$, k_{off} = 0.35 min^{-1}. These "expected" values were then compared to the experimental results shown in Figs. 6–8 ("observed").

	Percentage of [^{3}H]NMS binding to			Total binding (in % of equilibrium)
	A sites[a]	B sites[b]	C sites[c]	
Equilibrium				
Expected	47	33	20	(100)
Observed	43	n.d.	17	(100)
Pulse				
Expected	55	17	28	47
Observed	57	n.d.	25–30	47 ± 4
Pulse-chase				
Expected	55	44	1	14
Observed	52	48		17 ± 1

[a] Binding to A receptors was defined experimentally as [^{3}H]NMS labeling of sites with high affinity for unlabeled pirenzepine.

[b] Binding to B receptors was calculated but not measured experimentally (n.d.) since none of the molecules studied was B/A, C selective.

[c] Binding to C receptors was defined experimentally as [^{3}H]NMS labeling of sites with higher affinity for AF-DX 116, or (in pulse and pulse-chase experiments) as [^{3}H]NMS labeling of sites with higher affinity for AF-DX 116 and lower affinity for 4-DAMP and dicyclomine.

physiological conditions are, however, needed to confirm this hypothesis.

Biochemical implications of [^{3}H]NMS kinetic properties. [^{3}H]NMS binding to and dissociation from brain but not cardiac muscarinic receptors is clearly biphasic (Ref. 10).[2] Our results suggest that these complex kinetics reflected sequential association to and dissociation from C, A, and then, B receptors. Two experimental results support this hypothesis: 1) competition curves obtained after 1-min incubations with [^{3}H]NMS and the effect of 12-min dissociation on [^{3}H]NMS binding to A, B, and C receptors were compatible with the kinetic constants shown in Table 2; 2) competition curves obtained after pulse and pulse-chase incubations indicated that short association or dissociation periods favored [^{3}H]NMS binding to or dissociation from AF-DX 116-preferring (C) sites followed by pirenzepine-preferring (A) and then, AF-DX 116 and pirenzepine low affinity (B) sites.

In conclusion: 1) our data confirmed that [^{3}H]NMS, a so-called "nonselective" antagonist tracer, detected the existence of three binding sites with high affinities for atropine, slightly different [^{3}H]NMS affinity constants, and different kinetic constants.

2) These three binding sites presented a selectivity reminiscent of, respectively, muscarinic receptors responsible for K^+ conductance decrease in the nervous system, smooth muscle contraction in the ileum, and contractility inhibition in heart. This suggests that [^{3}H]NMS labeled selectively three functionally different receptors, possibly responsible for different muscarinic effects, in rat brain.

3) Sequential [^{3}H]NMS binding to these three receptors explained biphasic association and dissociation rates observed with this tracer in cortex homogenates.

[2] M. Waelbroeck, M. Gillard, P. Robberecht, and J. Christophe, unpublished data.

Acknowledgments

We thank Dr. A. Giachetti (Institute di Angeli, Milano, Italy) for helping us to obtain AF-DX 116 from Dr. K. Thomae GmbH (Biberach, FRG).

References

1. Barlow, R. B., K. J. Berry, P. A. M. Glenton, N. M. Nikolaou, and K. S. Soh. A comparison of affinity constants for muscarine-sensitive acetylcholine receptors in guinea-pig atrial pacemaker cells at 29°C and in ileum at 29°C and 37°C. *Br. J. Pharmacol.* **58**:613–620 (1976).
2. Mutschler, E., and G. Lambrecht. Selective muscarinic agonists and antagonists in functional tests. *Trends Pharmacol. Sci.* **5**(suppl.):39–44 (1984).
3. Stockton, J. M., N. J. M. Birdsall, A. S. V. Burgen, and E. C. Hulme. Modification of the binding properties of muscarinic receptors by gallamine. *Mol. Pharmacol.* **23**:551–557 (1983).
4. Mitchelson, F. Heterogeneity in muscarinic receptors: evidence from pharmacologic studies with antagonists. *Trends Pharmacol. Sci.* **5**(suppl.):12–16 (1984).
5. Giachetti, A., R. Micheletti, and E. Montagna. Cardioselective profile of AF-DX 116, a muscarine M_2 receptor antagonist. *Life Sci.* **38**:1663–1672 (1986).
6. Anwar-ul, S., H. Gilani, and L. B. Cobbin. The cardio-selectivity of himbacine: a muscarine receptor antagonist. *Naunyn-Schmiedeberg's Arch. Pharmacol.* **332**:16–20 (1986).
7. Giachetti, A., and R. Hammer. Hammer and Giachetti reply. *Trends Pharmacol. Sci.* **6**:358–359 (1985).
8. Hammer, R., C. P. Berrie, N. J. M. Birdsall, A. S. V. Burgen, and E. C. Hulme. Pirenzepine distinguishes between different subclasses of muscarinic receptors. *Nature (Lond.)* **283**:90–92 (1980).
9. Giraldo, E., R. Hammer, and H. Ladinsky. Binding profile in rat brain of compound AF-DX 116, a novel cardioselective muscarinic receptor antagonist of the competitive type. *Trends Pharmacol. Sci.* **7**(suppl.):80 (1986).
10. Waelbroeck, M., M. Gillard, P. Robberecht, and J. Christophe. Kinetic studies of [^{3}H]-*N*-methylscopolamine binding to muscarinic receptors in the rat central nervous system: evidence for the existence of three classes of binding sites. *Mol. Pharmacol.* **30**:305–314 (1986).
11. Birdsall, N. J. M., A. S. V. Burgen, R. Hammer, E. C. Hulme, and J. Stockton. Pirenzepine—a ligand with original binding properties to muscarinic receptors. *Scand. J. Gastroenterol.* **15**(suppl. 66):1–4 (1980).
12. Hammer, R., E. Giraldo, G. B. Schiavi, E. Monferini, and H. Ladinsky. Binding profile of a novel cardioselective muscarine receptor antagonist, AF-DX 116, to membranes of peripheral tissues and brain in the rat. *Life Sci.* **38**:1653–1662 (1986).
13. Nilvebrant, L., and B. Sparf. Dicyclomine, benzhexol and oxybutynine distinguish between subclasses of muscarinic binding sites. *Eur. J. Pharmacol.* **123**:133–143 (1986).
14. Nilvebrant, L., and B. Sparf. Differences between binding affinities of some antimuscarinic drugs in the parotid gland and those in the urinary bladder and ileum. *Acta. Pharmacol. Toxicol.* **53**:304–313 (1983).
15. Lowry, O. H., N. J. Rosebrough, A. L. Farr, and R. J. Randall. Protein measurement with the Folin phenol reagent. *J. Biol. Chem.* **193**:265–275 (1951).
16. Richardson, A., and A. L. Humrich. A microcomputer program for the analysis of radioligand binding curves and other dose-response data. *Trends Pharmacol. Sci.* **5**:47–49 (1984).
17. Cheng, Y., and W. H. Prusoff. Relationship between the inhibition constant (K_i) and the concentration of inhibitor which causes a 50 percent inhibition of an enzyme reaction. *Biochem. Pharmacol.* **22**:3099–3108 (1973).
18. Brunner, F., M. Waelbroeck, and J. Christophe. Secoverine is a nonselective muscarinic antagonist on rat heart and brain receptors. *Eur. J. Pharmacol.* **127**:17–25 (1986).
19. Waelbroeck, M., P. Robberecht. P. De Neef, and J. Christophe. Effects of *d*-tubocurarine on rat cardiac muscarinic receptors: a comparison with gallamine. *J. Recept. Res.*, in press.
20. Gillard, M., M. Waelbroeck, and J. Christophe. Muscarinic receptor heterogeneity in rat central nervous system. II. Brain receptors labeled by [^{3}H] oxotremorine-M correspond to heterogeneous M2 receptors with very high affinity for agonists. *Mol. Pharmacol.* **32**:100–108 (1987).
21. Gillard, M., M. Waelbroeck, and J. Christophe. *In vitro* effects of gallamine on dissociation kinetics of [^{3}H]*N*-methylscopolamine and [^{3}H]pirenzepine from rat brain muscarinic receptors. *J. Recept. Res.* **6**:47–61 (1986).
22. North, R. A. Muscarinic receptors and membrane ion conductances. *Trends Pharmacol. Sci.* **7**(suppl.):19–22 (1986).
23. Suprenant, A. Muscarinic receptors in the submucous plexus and their roles in mucosal ion transport. *Trends Pharmacol. Sci.* **7**(suppl.):23–27 (1986).

Send reprint requests to: Professor Jean Christophe, Department of Biochemistry and Nutrition, School of Medicine, Université Libre de Bruxelles, Boulevard de Waterloo 115, B-1000 Brussels, Belgium.